Molecular Biology of the Cell
Vol. 19, 1450–1461, April 2008

Different Effects of *Tetrahymena IFT172* Domains on Anterograde and Retrograde Intraflagellar Transport

Che-Chia Tsao and Martin A. Gorovsky

Department of Biology, University of Rochester, Rochester, NY 14627

Submitted May 3, 2007; Revised December 5, 2007; Accepted January 8, 2008
Monitoring Editor: Stephen Doxsey

Intraflagellar transport (IFT) particles are multiprotein complexes that move bidirectionally along the cilium/flagellum. The *Tetrahymena IFT172* gene encodes a protein with an N-terminal WD domain (WDD) and a C-terminal repeat domain (RPD). Epitope-tagged Ift172p localized to the basal body and in cilia along the axoneme, and *IFT172* knockout cells lost cilia and motility. Using serial deletion constructs to rescue the knockout cells, we found that neither the WDD nor the RPD alone is sufficient to assemble cilia. Ift172p containing only the WDD or the RPD failed to enter cilia. Constructs with a partial truncation of the RPD still rescued although cilia were assembled less efficiently, indicating that the WDD and a part of the RPD are sufficient for anterograde transport. Partial truncation of the RPD caused the accumulation of truncated Ift172p itself and of Ift88p at ciliary tips, suggesting that IFT turnaround or retrograde transport was affected. These results implicate different regions of Ift172p in different steps of the IFT process.

INTRODUCTION

Cilia and flagella are microtubule (MT)-containing organelles protruding from the cell surface that generate repetitive beating motility and/or function as sensors (Sleigh, 1974; Rosenbaum and Witman, 2002). The scaffold of these organelles, the axoneme, contains nine sets of MT doublets arranged as a hollow cylinder. At the base of the axoneme is the basal body, a MT-organizing center that contains nine sets of MT triplets. The plus ends of the axonemal MTs are in the distal tip of the cilium and the minus ends are at the proximal region near the basal body. Because ribosomes are not detectable within cilia, and assembly occurs largely, if not entirely, at the ciliary tip, all of the proteins required to assemble the axoneme must be imported from the cell body and transported up the cilium (Johnson and Rosenbaum, 1992).

Intraflagellar transport (IFT) is a bidirectional process that moves protein complexes (IFT particles) along the axoneme between the ciliary membrane and the outer doublet MTs (Kozminski *et al.*, 1993). IFT is essential to build cilia (Pazour *et al.*, 2000, 2002; Brazelton *et al.*, 2001; Deane *et al.*, 2001; Haycraft *et al.*, 2001, 2003; Brown *et al.*, 2003; Sun *et al.*, 2004; Hou *et al.*, 2007; Qin *et al.*, 2007) and to regulate ciliary length (Marshall and Rosenbaum, 2001; Marshall *et al.*, 2005). IFT machinery is also involved in cell signaling (Haycraft *et al.*, 2005; Huangfu and Anderson, 2005; May *et al.*, 2005; Wang *et al.*, 2006) and cell cycle control (Qin *et al.*, 2007; Robert *et al.*, 2007). Before entering cilia, IFT particles, MT motor proteins, and other cargos form complexes and dock at the basal body region (Deane *et al.*, 2001; Iomini *et al.*, 2001; Pedersen *et al.*, 2006). Anterograde IFT, mediated by kinesin-2 (Lawrence *et al.*, 2004), a heterotrimeric MT plus end-motor (Cole *et al.*, 1993), moves these complexes from the cell body to the ciliary tip where axoneme assembly occurs (Kozminski *et al.*, 1995; Pan *et al.*, 2006). At the tip region, the IFT complex is "remodeled": the IFT complexes dissociate from the MT, interact with ciliary tip proteins, unload their cargo, pick up disassociated axonemal components to be recycled, and activate a new motor protein, cytoplasmic dynein 1b, for retrograde transport back to the cell body (Pedersen *et al.*, 2003, 2005, 2006; Qin *et al.*, 2004). Genetic and phenotypic studies on mutants of IFT motor proteins showed that a defect in anterograde IFT results in complete failure to assemble cilia or in short cilia (Kozminski *et al.*, 1995; Brown *et al.*, 1999b; Sarpal *et al.*, 2003; Snow *et al.*, 2004), whereas a malfunction in retrograde IFT usually causes accumulation of IFT particles and ciliary proteins at ciliary tips (Pazour *et al.*, 1998, 1999; Signor *et al.*, 1999; Wicks *et al.*, 2000).

IFT particles purified from the green alga *Chlamydomonas reinhardtii* contain at least 16 protein components whose orthologues are conserved in organisms with cilia/flagella (Cole *et al.*, 1998). During purification, the IFT particles dissociate into two complexes, A and B (Cole *et al.*, 1998), which have been shown to have roles in the retrograde and anterograde processes, respectively (Iomini *et al.*, 2001; Scholey, 2003; Pedersen *et al.*, 2006). Most of the IFT proteins possess one or several domains implicated in protein–protein interactions (Cole, 2003), but the actual functions of these domains in the IFT process are not clear. *IFT172*, a complex B protein, is the IFT protein with the highest molecular weight (Cole *et al.*, 1998). In *Caenorhabditis elegans*, mutations in the *IFT172* ortholog, *OSM-1*, caused a defect in amphid sensory cilia (Perkins *et al.*, 1986; Bell *et al.*, 2006). In the *Chlamydomonas fla11* strain, a mis-sense mutation in *IFT172* led to flagella resorption at nonpermissive temperature (Pedersen *et al.*, 2005). A screen of zebrafish mutants with kidney cysts identified a mutation in *IFT172*, presumably affecting renal cilia formation (Sun *et al.*, 2004).

This article was published online ahead of print in *MBC in Press* (http://www.molbiolcell.org/cgi/doi/10.1091/mbc.E07–05–0403) on January 16, 2008.

Address correspondence to: Martin A. Gorovsky (goro@mail.rochester.edu).

Abbreviations used: HA, hemagglutinin; IFT, intraflagellar transport; LIM-ID, LIM-homeodomain transcription factor interaction domain; MT, microtubule; RPD, repeat domain; WDD, WD domain.

Interestingly, mammalian *IFT172* orthologues were identified without knowledge of their ciliary role. The rat orthologue, SLB, was identified as a selective Lhx3/4 LIM-homeodomain transcription factor binding protein and was shown to regulate the activities of Lhx3 in cultured cells (Howard and Maurer, 2000). The mouse *wimple* mutant, which is caused by a mis-sense mutation in the conserved C-terminal region of *IFT172*, had phenotypes similar to defects in the hedgehog signaling pathway (Huangfu *et al.*, 2003).

Ciliated protozoa in general, and *Tetrahymena thermophila* in particular, possess elaborate MT systems, including hundreds of cilia and basal bodies (Gaertig, 2000). With facile reverse genetic approaches to disrupt or replace target genes by homologous recombination (Hai *et al.*, 2000), *Tetrahymena* serves as an excellent model to dissect the structural and functional relationship of ciliary proteins. Here we report the cloning and characterization of *Tetrahymena IFT172*. Knockout of *IFT172* abolished ciliary assembly. By testing the ability of different truncation constructs to rescue *IFT172* knockout cells, we mapped the essential domains of *IFT172* for ciliary biogenesis. Phenotypic analyses of the rescued cells expressing different truncation forms of *IFT172* indicate that different regions of Ift172p play distinct roles in different steps of IFT.

MATERIALS AND METHODS

Tetrahymena Strains, Culture Growth, and Conjugation

Wild-type CU428 and B2086 strains of *T. thermophila* were provided by Dr. Peter Bruns (Cornell University). *IFT172* knockout strains were grown in MEPP medium (Orias and Rasmussen, 1976) at 30°C, and all the other cells used in this study were grown in 1× super protease peptone (SPP) medium (Gorovsky *et al.*, 1975) containing 1% peptone at 30°C. For starvation, midlog-phase cells were washed and resuspended in 10 mM Tris-Cl (pH 7.5) for 16–20 h at 30°C. For conjugation, equal numbers of the starved cells from two different mating types were mixed together and incubated at 30°C without shaking.

Deciliation and Cilia Regeneration

Cells were grown to midlog-phase, starved and deciliated by pH shock, and allowed to regenerate cilia as described (Calzone and Gorovsky, 1982).

Subtractive Hybridization Screening

Total RNA was prepared using Trizol reagent (Invitrogen, Carlsbad, CA) from starved *Tetrahymena* cells immediately after deciliation (0 h) or from cells incubated in cilia regeneration buffer for 1 h. Poly(A)$^+$ RNA was isolated using the Oligotex mRNA purification kit (Qiagen, Chatsworth, CA). Subtraction was based on a suppression PCR strategy (Gurskaya *et al.*, 1996) using the Clontech PCR-Select cDNA subtraction kit (Clontech, Palo Alto, CA) mainly following the manufacturer's protocol as previously described (Dou *et al.*, 2005). The 0-h mRNA was used as the "driver" and 1-h cilia regeneration mRNA as the "tester"; the ratio of driver to tester was 5:1 with additional SerJ-like cDNA added into the driver pool. The suppression PCR products were cloned into the SmaI site on the pBluescript KS II vector (Stratagene, La Jolla, CA) by blunt-end ligation and sequenced from one end using the M13-reverse primer. cDNA sequences were BLAST searched against the NCBI GenBank database to identify possible orthologues.

Gene Cloning and Sequence Analysis

Genomic DNA was extracted from CU428 cells as previously described (Liu *et al.*, 2004). The *Tetrahymena IFT172* gene sequence was determined by a genomic walking method (Liao *et al.*, 1997). To determine the coding sequence, mRNA from 1-h cilia regeneration cells was reverse-transcribed with SuperScript II reverse transcriptase (Invitrogen) following the manufacturer's instructions. The cDNA sequence was compared with the genomic DNA sequence to verify the exon-intron determinations. The GenBank accession number of *IFT172* is EF495115.

The consensus secondary structure was predicted by NPS@PBIL-IBCP (http://npsa-pbil.ibcp.fr). The protein motif and repeat identification were done using SMART (Schultz *et al.*, 1998) and REP v1.1 (Andrade *et al.*, 2000), respectively. The multiple alignment was performed with CLUSTALX with default settings (Thompson *et al.*, 1997).

Knockout, Rescue, and Expression Constructs

A genomic sequence containing 0.6 kb upstream and 1.8 kb downstream of the *IFT172* coding region was obtained by PCR using Pfu turbo enzyme (Invitrogen, Carlsbad, CA) and cloned into the SmaI site on the pBluescript KS II vector to create the pRFT2 construct. Using pRFT2 as template and two outward primers annealing to the 5′ noncoding region or to the 3′ region of the *IFT172* coding sequence, a PCR fragment containing the vector and 5′ and 3′ noncoding regions was amplified, kinased, and circularized by blunt-end ligation to a *neo3* cassette (Shang *et al.*, 2002b) to create the *IFT172* knockout construct, in which 5.9 kb of the *IFT172* coding sequence was replaced by the cassette. This construct also carried 0.6- and 1.8-kb flanking regions at the 5′ and 3′ ends, respectively, for homologous gene targeting (see Figure 2A).

The pRFT2 plasmid was used to create rescue constructs targeting to the *IFT172* locus. Different truncated forms of *IFT172* were obtained by PCR (see Supplementary Materials for primers used), and a C-terminal HA epitope was introduced by adding the corresponding nucleotide sequences into the 3′ primers. A pTTMet construct (Shang *et al.*, 2002b) was used to create rescue constructs targeting to the *MTT1* locus. The *MTT1* coding sequence on pTTMet was replaced by different truncated forms of *IFT172* amplified from genomic DNA by PCR, and the C-terminal FLAG epitope was introduced by adding the corresponding nucleotide sequences into the 3′ primers.

The expression construct (see Figure 3B) was modified from the rescue construct targeting to the *MTT1* locus. A *neo2* selectable marker (Gaertig *et al.*, 1994) was inserted into the AccI site of the 5′ *MTT1* flanking region as previously described (Dou *et al.*, 2005).

Germline Knockout

The germline knockout strains were generated as described (Hai and Gorovsky, 1997). The targeting DNAs were released by SacII and XhoI from the knockout construct and introduced into conjugating CU428 and B2086 cells by biolistic particle bombardment 3 h after mixing (Cassidy-Hanley *et al.*, 1997). The germline transformants were selected, assorted, and made homozygous in the micronucleus by Round I genomic exclusion (Hai and Gorovsky, 1997). Both the star and nonstar side of the exconjugants were used as parental heterokaryon cells to generate homozygous homokaryon knockout progeny cells.

To assay the knockout phenotype, starved knockout heterokaryon cells were mixed to induce conjugation, and individual conjugating pairs were isolated and transferred into drops of SPP medium in a Petri dish between 6 and 10 h after mixing. After 2 d, progeny cells were transferred to microtiter plates and further selected with 120 μg/ml paromomycin sulfate and 1 μg/ml $CdCl_2$ in MEPP medium to eliminate the paromomycin-sensitive cells derived from aborted conjugants. The true *IFT172* knockout progeny were maintained in MEPP medium with vigorous shaking and examined with an Olympus SZH-ILLD dissecting microscope (Melville, NY).

Rescue of the IFT172 Knockout Cells

Nonmotile *IFT172* knockout cells were grown in MEPP medium with vigorous shaking and washed with 10 mM Tris-Cl (pH 7.5) before transformation. The targeting DNA fragments were released from the cloning vector by restriction digestion and were introduced into the cells by biolistic transformation as previously described (Cassidy-Hanley *et al.*, 1997). After bombardment, cells were incubated in 75 ml of SPP medium with gentle shaking at 30°C for 3 h before aliquoting into microtiter plates. When *MTT1* promoter-driven expression was required, 1 μg/ml $CdCl_2$ was added into the medium immediately after transformation. The rescued swimming cells were identified using an Olympus SZH-ILLD dissecting microscope 3 d after transformation. Each construct was used for at least three independent transformation trials with a full-length wild-type construct as a positive control. pBluescript plasmid was used as a negative control. Constructs that failed to give swimming transformants in three attempts where the positive controls gave rescued cells were regarded as nonrescuing constructs.

Epitope Tagging

To generate epitope-tagged, C-terminal repeat domain (RPD)-truncated knockin strains, the C-terminal FLAG or hemagglutinin (HA)-tagged *IFT172* constructs were introduced into the *IFT172* knockout cells by the rescuing strategy described above.

To localize Ift172p with WD domain (WDD) or RPD mutations in the cells expressing Ift72p from the wild-type locus, the FLAG-tagged expression constructs were digested with XhoI and SacII and introduced into starved, full-length *IFT172*-rescued cells by biolistic transformation. After bombardment, the cells were incubated in SPP medium at 30°C with gentle shaking for 3 h and subsequently plated into microtiter plates. The transformants were initially selected with 120 μg/ml paromomycin and maintained in 250 μg/ml paromomycin in SPP medium. To induce the expression of FLAG-tagged WDD or RPD, cells were grown in SPP medium with 0.05, 0.2, 0.5, 1, and 2 μg/ml $CdCl_2$ for at least 6 h.

To make *IFT88*-GFP strains, a targeting construct containing the *IFT88* coding region (*Tetrahymena* Genome Database ID 252.m00027) fused with a GFP sequence at the C-terminus upstream to the termination codon was

created by overlapping PCR (see Supplementary Material for primers used). For selecting the transformants, a *MTT1* promoter-driven cassette (J. Bowen and M. A. Gorovsky, personal communication) containing the cycloheximide-resistant *rpl29(K40M)* gene (Yao and Yao, 1991) was included between the green fluorescent protein (GFP) and *IFT88* 3′ flanking region. The tagged construct was transformed into *IFT172* knockout cells that had been rescued either with full-length *IFT172* or with *IFT172* truncated form IFT172 (RPDΔ3; see Figure 5A). After biolistic bombardment, the cells were incubated with SPP containing 1 μg/ml $CdCl_2$ for 4 h at 30°C followed by adding 5 μg/ml cycloheximide into the medium at room temperature overnight. Before aliquoting the cells onto microtiter plates, additional cycloheximide was added to the medium to make the final concentration 15 μg/ml. The cells were incubated and selected at 30°C. Fluorescent microscopy was used to observe Ift88p-GFP localization in cells fixed with 0.05% formaldehyde in 10 mM Tris-Cl (pH. 7.5) at room temperature for 5 min.

Southern Analysis and Genomic PCR

Genomic DNA was digested with NsiI at 37°C overnight and electrophoresed on 0.8% agarose gel. The DNA was denatured and blotted to MagnaGraph membrane (Osmonics, Trevose, PA) as described (Liu *et al.*, 2004). To make a probe, a coding region corresponding to a 5′ part of the open reading frame was amplified by PCR, purified, and labeled by random priming with [α-^{32}P]dATP. The blot was hybridized at 42°C overnight as described (Liu *et al.*, 2004), washed, and exposed to x-ray film. To analyze the genotype of the transformed *Tetrahymena*, genomic DNA was used as template and was analyzed by PCR with locus-specific primers, using TripleMaster enzyme mix (Eppendorf, Fremont, CA).

Northern Analysis

Total RNAs were extracted with Trizol reagent (Invitrogen) from midlog-phase cells and from deciliated cells incubated in cilia regeneration buffer for 0, 1, or 2 h. Twenty micrograms total RNA was resolved on 2.2 M formaldehyde-1% agarose gels and blotted to MagnaGraph membrane (Osmonics). The hybridization was performed at 42°C overnight in hybridization buffers containing 50% formamide as previously described (Dou *et al.*, 2005) with the same DNA probe used for Southern analysis.

Measuring Swimming Path

Fifteen microliters of cell culture were spread on a glass slide to make a thin spot (diameter ~15 mm) and were allowed to sit and adapt for 5 min. Swimming paths were recorded using an Olympus BH-2 microscope with dark-field 4× objective with a 2-s exposure on Kodak film (Eastman Kodak, Rochester, NY). The negatives were scanned and path lengths were measured using NIH ImageJ Software (version 1.3; http://rsb.info.nih.gov/ij/).

Ink Particle Uptake Assay

Cells were washed and resuspended in 10 mM Tris (pH 7.5). A drop of Higgins India black ink was added (~1 μl ink per ml of cells), and the cells were kept at 30°C with gentle shaking for at least 30 min. Cells were fixed with 10% Formalin and examined using a bright-field Olympus BH-2 microscope.

Immunofluorescent Staining

To stain FLAG-tagged strains, cells were fixed with 2% paraformaldehyde, 0.5% Triton X-100 in PHEM buffer (60 mM PIPES, 25 mM HEPES, 10 mM EGTA, 2 mM $MgCl_2$, pH 6.9) for 1 min at room temperature and immediately were washed with 1% bovine serum albumin (BSA) in phosphate-buffered saline (PBS) and treated in 45% ethanol-0.5% Triton X-100 on ice overnight. To stain all other cell strains used in this study, cells were fixed with 2% paraformaldehyde in PHEM buffer for 1 h as described (Stuart and Cole, 2000). The fixed cells were spread on 0.01% poly-L-lysine–coated cover glasses and blocked with 10% normal goat serum and 3% BSA in PBS with 0.1% Tween-20 at 37°C for 30 min. After blocking, the cells were incubated with primary antibodies [rabbit anti-tubulin, 1:1000 (Van De Water *et al.*, 1982); rabbit anti-polyglycine serum (Xie *et al.*, 2007), rabbit anti-polyglutamine serum (Shang *et al.*, 2002a), mouse anti-HA, or mouse anti-FLAG antibody, 1:500] at room temperature for 1 h or at 4°C overnight, followed by incubating with secondary antibodies (goat anti-rabbit IgG FITC conjugant, 1:500; goat anti-mouse IgG+M Alexa 595 conjugants, 1:500) at room temperature for 1 h. For staining nuclei, the slides were incubated with PBS-0.1% Tween-20 with 10 ng/ml DAPI (Roche, Indianapolis, IN) for 10 min after secondary antibody incubation. The slides were mounted with DABCO (Sigma, St. Louis, MO) and observed with a Leica TCS SP confocal microscope (Deerfield, IL), or Olympus BH-2 fluorescent microscope (Melville, NY). The overlaid images were processed by Adobe Photoshop 7.0 (San Jose, CA).

RESULTS

Isolation and Cloning of Tetrahymena IFT172

Tetrahymena deciliated by a pH shock combined with shearing force rapidly regenerate cilia in a recovery buffer (Rosenbaum and Carlson, 1969; Guttman and Gorovsky, 1979). To explore the genes involved in cilia assembly and function, we used a subtractive hybridization approach to isolate genes whose transcripts were highly induced during cilia regeneration. A 572-base pair cDNA clone exhibited significant sequence similarity to rat SLB and *C. elegans OSM-1* (Cole *et al.*, 1998; Howard and Maurer, 2000), suggesting that it encodes the *Tetrahymena IFT172* ortholog. Southern analysis showed that the cDNA was derived from a single copy gene (data not shown). Using a chromosomal walking method, we assembled a 9.4-kb genomic sequence containing a 0.6-kb 5′ and a 1.8-kb 3′ flanking region. Subsequently when the draft sequence of the *Tetrahymena* macronuclear genome became available at The Institute for Genomic Research (http://www.tigr.org/tdb/e2k1/ttg/), we searched the whole genome and verified that the gene we cloned is the only sequenced *IFT172* homolog.

To define the structure of *IFT172*, we amplified the coding region of the cDNA using RT-PCR and compared it to the genomic DNA sequences, identifying at least 12 exons and 11 introns. The open reading frame encodes a protein of 1718 amino acid residues with predicted molecular weight of 197 kDa and pI of 6.9.

Ift172p Is a Conserved Protein with Distinct N-Terminal WD and C-Terminal Repeat Domains

Tetrahymena Ift172p shows ~39% identity and 61% similarity, respectively, to rat IFT172/SLB (Figure 1B). Sequence alignment showed that the homology extended throughout the entire coding region (see Supplementary Materials). Seven predicted WD40 motifs are located at the N-terminus (Figure 1A, black boxes), and the C-terminal region is composed of degenerate TPR-like repeats (Figure 1A, light gray boxes). Although the repeat units were not identical, they all contain a core consensus sequence $AX_{12}AX_2MYX_5(W/Y/F)X_2AX_3A$ (Pedersen *et al.*, 2005; Figure 1C). The distinction between the N- and C-terminal domains is reinforced by secondary structure predictions. The N-terminal region contains exclusively beta-strands and short random loops, whereas the C-terminal repeat region is composed of alpha helical structures connected with loops (Figure 1A). Furthermore, each C-terminal repeat unit could be superimposed with three or four helices (Figure 1C), suggesting that they form a structural module. Homologues from other organisms share a similar domain organization (Figure 1B). That the sequence varies in each repeat unit but can be aligned with orthologues from different species suggests that different repeats might be functionally distinct. Supporting this, in rat SLB, the region responsible for interaction with the LIM-homeodomain transcription factor Lhx3 has been mapped to residues 1213-1265 (Howard and Maurer, 2000). Using this rat sequence to perform a BLAST similarity search against the whole *Tetrahymena* Ift172p sequence, we identified a region in *Tetrahymena* Ift172p, which corresponds to the tenth repeat (Figure 1A, dark gray box). The E-value for the matching tenth repeat was smaller by two orders of magnitude than that for the next best repeat. Therefore, three distinct regions can be identified in *Tetrahymena* Ift172p: the N-terminal WDD, the RPD, and a single repeat unit that aligns with and is highly homologous to the LIM-interaction domain (LIM-ID) on rat SLB (Figure 1A).

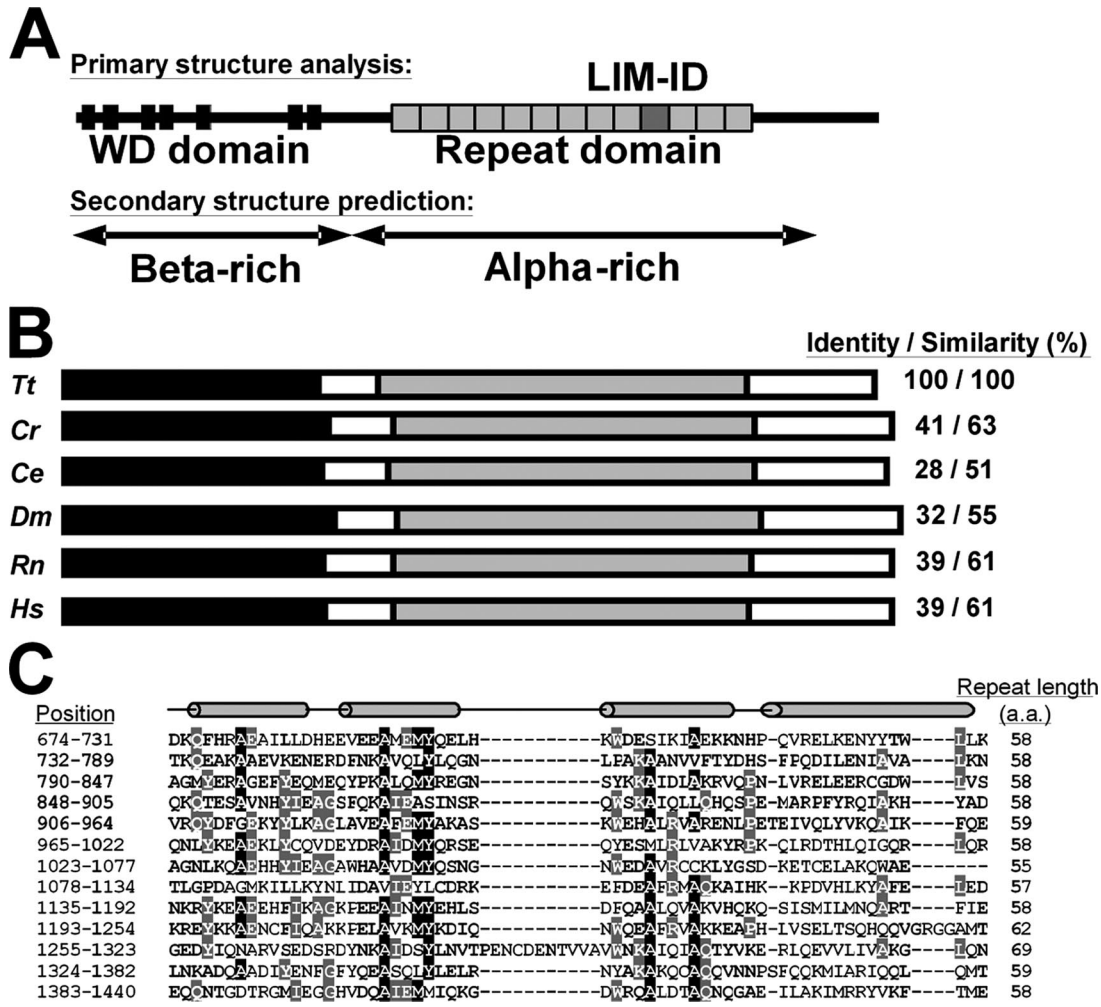

Figure 1. Features of the *Tetrahymena IFT172* gene sequence. (A) Secondary structure prediction and domain organization of Ift172p. Black boxes indicate 7 WD motifs. Light gray boxes show 13 degenerate repeat units. The dark gray box indicates the repeat unit which is aligned and homologous to the LIM-transcription factor interaction domain (LIM-ID) of rat SLB/IFT172. (B) Comparison of *Tetrahymena* Ift172p and orthologues from different species. The overall sequence identity and similarity were compared with *Tetrahymena* Ift172p. *Tt, Tetrahymena thermophila*, EF495115; *Cr, Chlamydomonas reinhardtii*, AAT99263.1; *Ce, Caenorhabditis elegans*, NP_510681.2; *Dm, Drosophila melanogaster*, NP_647700.1; *Rn, Rattus norvegicus*, NP_446244.1; *Hs, Homo sapiens*, NP_056477.1. (C) Sequence alignment of *Tetrahymena* Ift172p repeat units. Black and gray shadings show conserved residues with 60 or 35% identity, respectively. The predicted alpha helices are shown as cylinders above the alignment.

IFT172 Is Required for the Assembly and Function of Somatic and Oral Cilia

To study the in vivo function of *IFT172*, we generated germline knockout cells by homologous recombination using standard *Tetrahymena* genetic methods (Hai *et al.*, 2000). All of the *IFT172* coding sequences in both micronuclear and macronuclear genomes were disrupted with a *neo3* selection cassette (Figure 2A). Southern blotting analysis of the genomic DNA extracted from the knockout cells indicated that the original *IFT172* genes were completely replaced by disrupted constructs (Figure 2B). To further confirm that expression of *IFT172* had been abolished, we analyzed the *IFT172* message level from cells incubated in recovery buffer for different periods of time after deciliation. In wild-type cells, *IFT172* message was expressed at a very low level in vegetative growth but dramatically increased after 2 h of cilia regeneration (Figure 2C, WT), consistent with our subtractive screening result that *IFT172* is induced during cilia regeneration. In the *IFT172* knockout cells, however, no *IFT172* message could be detected by Northern analysis in vegetative growth, after pH shock or during incubation in recovery buffer (Figure 2C, KO), verifying that we have created *Tetrahymena* strains that cannot express *IFT172*.

The most prominent phenotype of *IFT172* knockout cells was the loss of normal motility and the ability to complete cytokinesis (see below). The knockout cells could not swim and settled at the bottom of the microtiter plates in which they were grown. Bright field microscopy revealed that the mutants were either nonmotile or only had limited trembling movement, indicating that their somatic cilia were absent or not functional.

We then analyzed the morphology of cells. Staining with anti-tubulin antibodies showed that wild-type cells had many long cilia (Figure 2D), whereas *IFT172* knockout cells lacked cilia or had only very short cilia (Figure 2, E and F). When cells were incubated without shaking, they could be categorized into three groups according to their morphology: discrete single cells, chains of two or more cells, and

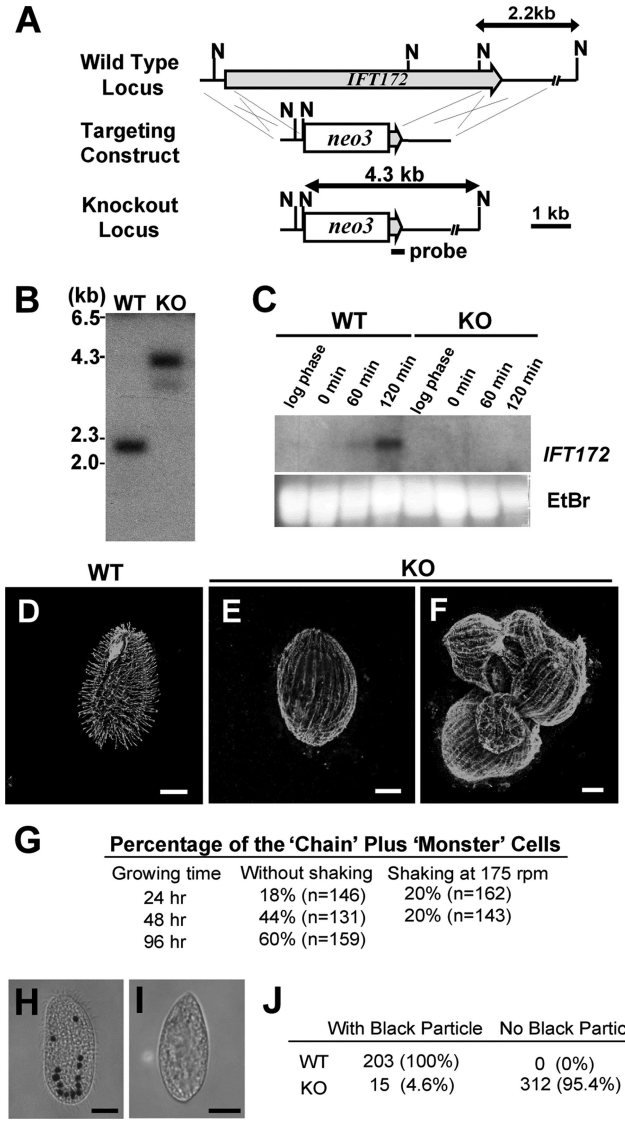

Figure 2. Construction and characterization of *IFT172* knockout cells. (A) Strategy to generate knockout cells. The wild-type locus of the *IFT172* gene was targeted with the disruption construct by homologous recombination, replacing most of the coding region with a *neo3* cassette in the knockout locus. Short bar, the probe for Southern analysis. N, NsiI site. (B). Southern blot analysis of the genotype. Genomic DNA extracted from CU428 wild-type strain and *IFT172* knockout strains was digested with NsiI and resolved on an agarose gel. The blot was probed with an isotope labeled *IFT172* cDNA fragment as indicated in A. The absence of the 2.2-kb band from the knockout cells (KO) shows that the wild-type *IFT172* gene (WT) is replaced by a knockout allele. (C) Northern analysis of *IFT172* expression during cilia regeneration. CU428 wild-type cells and *IFT172* knockout cells were treated with a pH shock and allowed to regenerate cilia. Total RNAs were extracted from log phase cells and from the cells collected at 0, 60, and 120 min after deciliation and probed with the *IFT172* cDNA probe. *IFT172* transcripts were highly induced during cilia regeneration in wild-type cells. No *IFT172* messages could be detected in knockout cells. The bottom panel shows the ethidium bromide staining to control for loading. (D–F). Morphology of wild-type and *IFT172* knockout cells. The cells were stained with anti-tubulin antibodies. Wild-type cells contain hundreds of cilia (D), but *IFT172* knockout cells cannot assemble normal length cilia (E and F). With the loss of ciliary beating, *IFT172* knockout cells fail to finish division, fuse, and form large, multinucleated monster cells (F). Bar, 10 μm. (G) Percentage of the chain cells and monster cells cultured with or without vigorous shaking. Culturing cells with shaking can partially rescue the cytokinesis defect of *IFT172* knockout cells. (H–J) Ink uptake assay to test oral cilia function. Black ink was added into the medium, and the numbers of cells that contained ink particles were measured after 4 h. Although all the wild-type cells contain large black food vacuoles (H), <5% of *IFT172* knockout cells form black vacuoles (I). Bar, 10 μm.

giant "monster" cells. The fraction of chain cells plus monster cells increased with time (from 18 to 60%, after 96 h, Figure 2G), and the number of discrete single cells gradually decreased (Figure 2G). This is consistent with the report that a ciliary defect in *Tetrahymena* can lead to a secondary phenotype in cytokinesis because nonmotile cells are unable to generate the twisting motion (rotokinesis) required for complete separation of daughter cells (Brown *et al.*, 1999a). Initially, these nonmotile cells become connected chains of cells. Subsequently the cells in a chain fused to form giant, multinucleated monsters and eventually die. If this is the case, culturing the cells with external shaking to break up the connected cells should rescue the phenotype. Indeed, when *IFT172* knockout cells were cultured with vigorous shaking, the fraction of the chain cells plus monster cells did not increase (Figure 2G). All of these observations argue that *IFT172* is essential for normal function of the somatic cilia.

In addition to somatic cilia, the *Tetrahymena* oral apparatus contains a high density of cilia whose beating is repetitive and generates fluid currents to facilitate food ingestion by phagocytosis (Frankel, 2000). In SPP medium, we found that *IFT172* knockout cells could only survive for a short time but became growth-arrested and then died. However, in MEPP medium, which stimulates endocytosis and allows cells to bypass the dependence of growth on functional oral cilia (Orias and Rasmussen, 1976), the mutant cells could divide about every 12 h for several days. This result suggested that *IFT172* is also required for functional oral cilia. To further test this, we added a drop of ink into the medium and measured the number of the cells that could ingest ink particles. After incubation with ink for 4 h, more than 99% of the wild-type cells (n = 203) had several black food vacuoles inside the body (Figure 2H), but <5% of *IFT172* knockout cells (n = 327) formed black vacuoles (Figure 2, I and J), suggesting that oral as well as somatic cilia need *IFT172* proteins for assembly or function.

IFT172 Proteins Are Enriched in Basal Bodies and Cilia

Because deletion of the *IFT172* gene causes a ciliary defect, reintroducing wild-type *IFT172* genes into knockout cells should rescue the phenotype (Figure 3A). To investigate this, we created rescue constructs containing an *IFT172* gene with a HA epitope tag at the C-terminus to enable the localization of Ift172p by immunostaining with anti-HA antibodies. Two types of rescue constructs were created to target the rescuing gene either to the endogenous *IFT172* locus (Figure 3B, Rescue construct), or to the nonessential metallothionein *MTT1* locus so that expression of the introduced gene could be induced by adding cadmium into the medium (Shang *et al.*, 2002b). Both targeting strategies gave similar results. Three days after transformation, some cells started to swim and began dividing rapidly, whereas no swimming cells were observed in the controls that had been transformed with vector alone. The *IFT172*-HA rescued cells grew and were morphologically similar to wild-type cells, indicating that the loss of cilia phenotype was indeed caused by deletion of *IFT172* and that the HA-tagged Ift172p was functional.

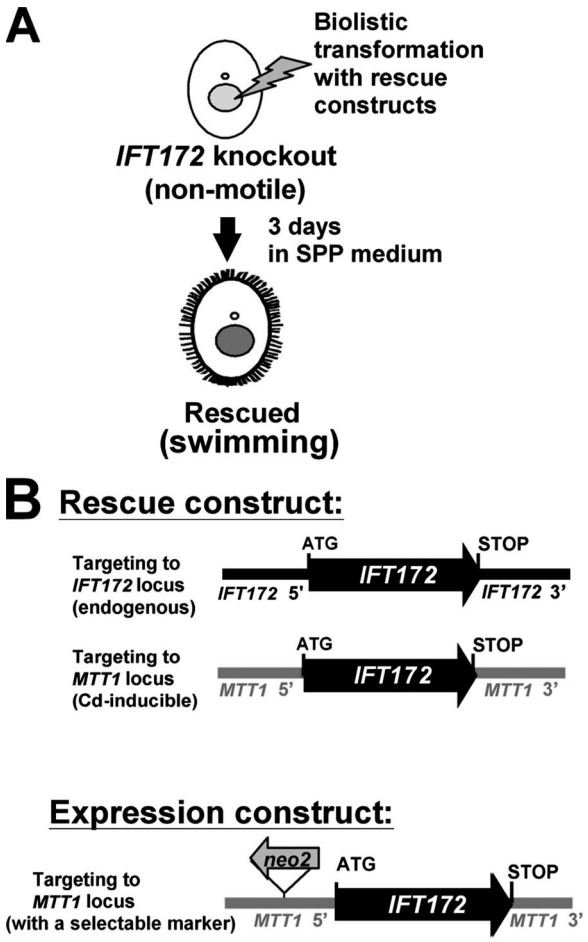

Figure 3. Rescue experiment. (A) Strategy to map the functional domains and generate "knock-in" mutant cells by rescue of motility using *IFT172* knockout cells. (B) Constructs for rescue experiments and for expressing Ift172p in the wild-type cells.

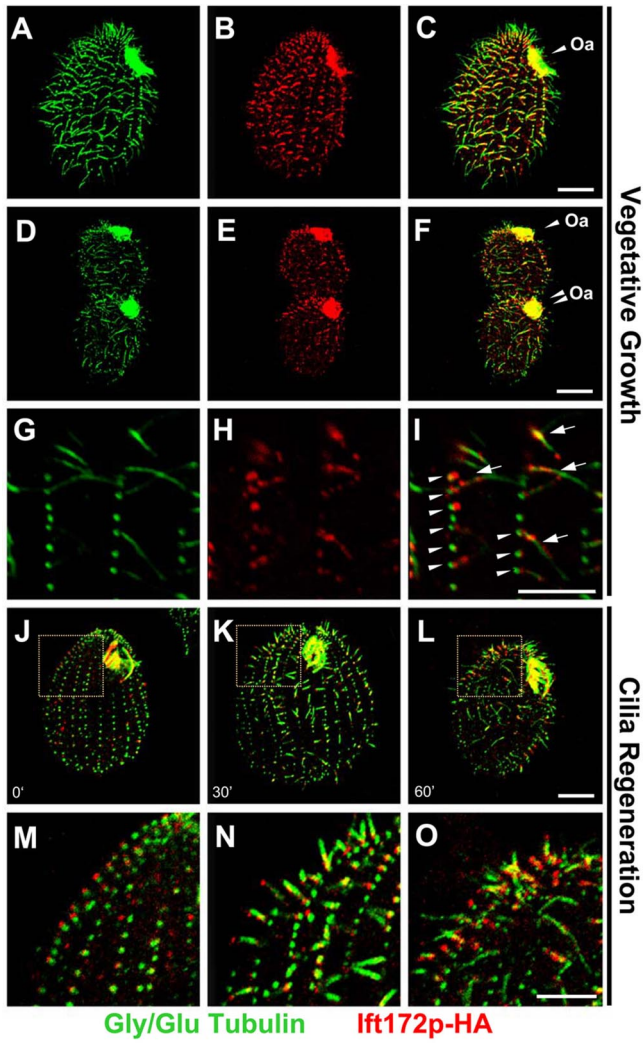

Figure 4. Localization of the Ift172p-HA. Confocal images of nondividing (A–C) and dividing (D–F) cells expressing *IFT172*-HA. The cells were stained with both anti-glutamylated and anti-glycylated tubulin antiserum (A and D, green) to visualize cilia and basal bodies and with anti-HA mAb (B and E, red) to detect Ift172p-HA. The overlay images (C and F, yellow) indicate that Ift172p localizes along the cilia and to the basal bodies. The oral apparatus (Oa), which has a high density of oral cilia, is stained strongly by anti-HA antibodies in both nondividing and dividing cells. The single arrowhead indicates the old oral apparatus, and the double arrowhead marks the newly formed oral apparatus in the dividing cell. Bar, 10 μm. (G–I) High-magnification images to show that Ift172p-HA (red) localized to the cilia (arrow) and is closely associated with the basal body (arrowhead). Bar, 5 μm. (J–O) Merged confocal images of glutamylated/glycylated tubulin and Ift172p-HA staining on regenerating cilia. (M–O), enlarged images of the boxed regions shown in J–L, respectively. (J and M) Deciliated cells; (K and N) 30 min in the recovery buffer; (L and O) 60 min in the recovery buffer. Bar, 10 μm.

When we stained *IFT172*-HA cells with antibodies against glutamylated and glycylated tubulins to highlight the basal bodies and cilia (Figure 4, A, D, and G) and used anti-HA antibody to visualize tagged Ift172p (Figure 4, B, E, and H), we observed strong signals at the oral apparatus (Figure 4, C and F, Oa), which contains a high density of oral cilia. We also found Ift172p localized in the somatic cilia (Figure 4I, arrows) and closely associated with somatic basal bodies (Figure 4I, arrowheads). The HA staining was distributed in patches along the whole cilium, with a stronger signal at the proximal region (Figure 4, H and I, arrows). We did not detect Ift172p-HA staining in either the macronucleus or micronucleus during vegetative growth or cilia regeneration, indicating that little or no Ift172p is present in *Tetrahymena* nuclei (see *Discussion*).

In addition to observing ciliary staining in growing cells, we also investigated the Ift172p distribution within newly formed cilia at different time points during cilia regeneration. On deciliation, Ift172p-HA was seen at somatic basal bodies and at the base of oral cilia (Figure 4, J and M). After 30 min, we observed elevated Ift172p-HA signals in the short, newly formed cilia (Figure 4, K and N) with some strong staining at the distal region. The HA signals in the cilia decreased slightly after an hour, when regeneration was nearly finished (Figure 4, L and O). These observations indicate that *IFT172* is actively involved in the assembly of new cilia.

Both the WD and Repeat Domains Are Required for IFT172 to Assemble and Localize to the Cilia

Ift172p contains a distinct N-terminal WDD and a C-terminal RPD (Figure 1A). To study the role of these two domains, we created constructs that contained only the WDD or the

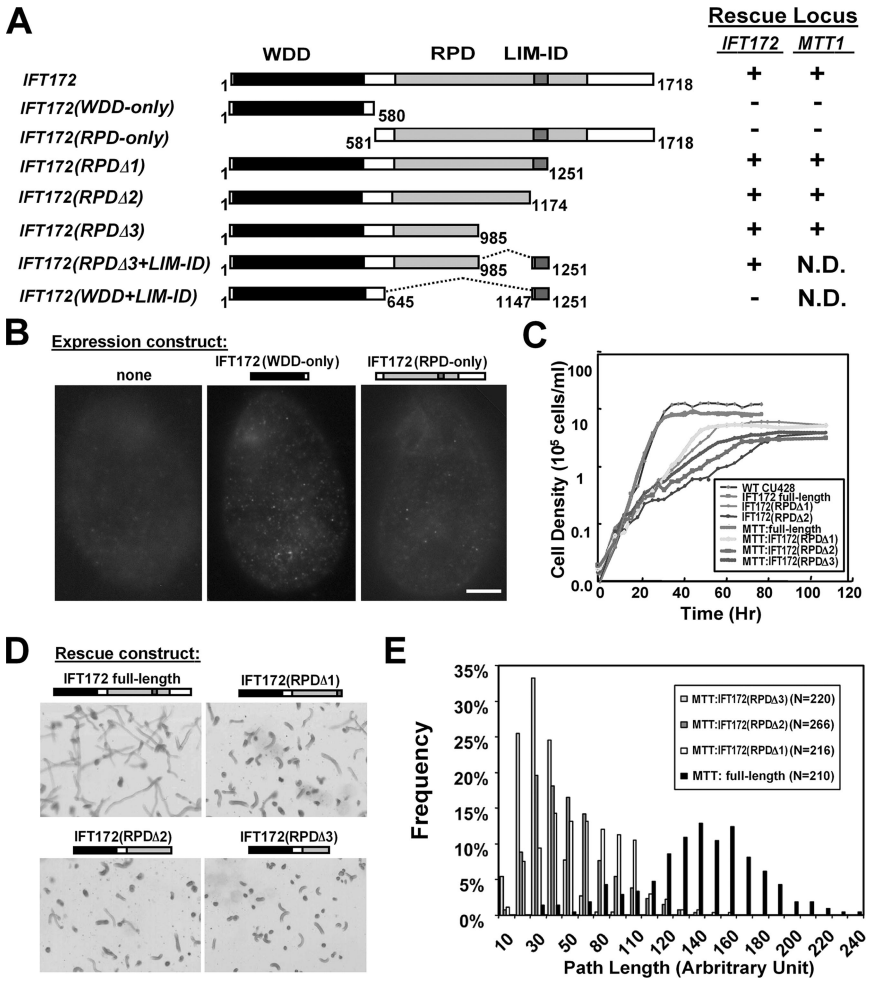

Figure 5. Phenotypic analyses of cells rescued with RPD deletion constructs. (A) Deletion constructs and rescue results. Black regions represent the WDD, gray regions represent the RPD, and the dark gray box indicates the repeat unit corresponding to LIM-ID. The amino acid residue numbers are labeled according to the full-length protein. +, the construct rescued the knockout cells; −, the construct failed to rescue. N.D., not determined. (B) Immunolocalization of the FLAG-tagged Ift172p WDD or PRD expressed in the wild-type CU428 cells. Untransformed CU428 was used as negative control for staining. Both truncated proteins showed punctate localization in the cytosol and did not appear in the cilia or basal body. Bar, 10 μm. (C). Growth curve of different cell lines rescued by deletion constructs. Solid lines show the cells rescued with constructs targeting to the *IFT172* endogenous locus. Dotted lines show cells in which the rescue constructs were targeted to the *MTT1* locus and the cells were grown with 1 μg/ml cadmium chloride in SPP medium. The rescued results are consistent between the two targeted loci. Although cells rescued by full-length *IFT172* had the same doubling time as CU428 wild-type cells, cells rescued by RPD truncated forms divided slower. (D) Negative images of the swimming paths of the cells rescued with four different truncation constructs. The paths were recorded by 2-s exposures of the swimming cells under low magnification with a dark-field microscope. The constructs used for rescue are shown above each image. (E) Frequency distribution of the path lengths measured from C.

RPD [Figure 5A, IFT172(WDD-only) and IFT172(RPD-only)] and tested whether they could restore ciliary assembly in the *IFT172* knockout cells. Although the full-length control construct could rescue the *IFT172* knockout phenotype, neither of the two single domain constructs could rescue in multiple transformations (Figure 5A). This result indicates that neither the WDD nor RPD of Ift172p alone is sufficient to assemble cilia.

To determine whether failure of the single domain constructs to rescue the nonmotile phenotype of *IFT172* knockout cells reflected a failure to localize to cilia or a failure to function after localization, WDD and RPD constructs that had a FLAG epitope fused to the C-terminus were targeted to the *MTT1* locus (Figure 3B, Expression construct). A flanking *neo2* selectable marker (Gaertig *et al.*, 1994) was included to select transformants when these constructs were introduced into wild-type cells. PCR analysis of the genomic DNA extracted from the selected transformed cells confirmed that the WDD and RPD constructs correctly targeted to the *MTT1* locus (not shown). After adding 0.5 μg/ml cadmium to induce the expression of truncated Ift172p, we examined localization of the FLAG-tagged proteins. We found that both the Ift172p WDD and RPD failed to localize to any specific subcellular structure (Figure 5B). The staining signals were punctate in the cytosol and were not present in cilia. We also examined the localization of these tagged proteins under more moderate induction conditions (0.05 and 0.2 μg/ml cadmium chloride for 4 h). The staining intensity varied, but the patterns were similar in those induction conditions. Therefore, the punctate localization is not likely due to the overexpression of the truncated proteins. These results suggest that both of the major domains are required for Ift172p to dock to the basal body and enter the cilia. Increasing the cadmium to 2 μg/ml did not affect the WDD-transformed or wild-type control cells after 6 h, but the RPD-transformed cells became round and died, suggesting that high level expression of RPD was toxic to the cells.

The WD Domain plus a Part of the C-Terminal Repeat Domain Are Sufficient for Cilia Assembly

To further analyze the function of the RPD, we created a series of deletion constructs in which various lengths of the RPD were deleted from the C-terminal end and tested the abilities of these constructs to rescue *IFT172* knockout cells (Figure 5A). We found that partial truncations of the RPD did not abolish the ability of Ift172p to assemble functional cilia [Figure 5A, IFT172(RPDΔ1)]. Additional deletions showed that the tenth repeat unit, which showed homology to and aligned with the LIM-ID on rat SLB (Howard and Maurer, 2000), also was not essential [Figure 5A, IFT172(RPDΔ2) and IFT172(RPDΔ3)]. These results indicate that only a small part of the RPD is required to work with the WDD to assemble functional cilia. Thus, the RPD repeats likely have redundant functions. More than one of the repeats, however,

may be required because fusion of the LIM-ID repeat alone to the WDD also did not rescue [Figure 5A, IFT172(WDD+LIM-ID)]. Given that cilia assembly is dependent on anterograde IFT to deliver the building materials to the tip (Qin *et al.*, 2004), these results suggest that much of the RPD, including the region corresponding to the conserved LIM-ID, is not required for anterograde transport.

We further examined the behavior and morphology of the *IFT172* knockout cells rescued by the partially truncated RPD constructs. Cells rescued by "knocking in" the truncated constructs could assemble cilia but did not completely recover wild-type function. These partially truncated *IFT172* RPD cells had longer doubling times (~6–11 h, Figure 5C) than the wild-type cells (~3 h) or than cells rescued with the full-length construct (~3 h). In addition, partially truncated *IFT172* RPD mutant cells also swam slower. When we spread the cells in a thin layer of medium on a glass slide and recorded the swimming paths, we found the path length of the truncated mutant cells to be much shorter than the full-length control (Figure 5D), and the swimming rate decreased in proportion to the extent of the deletion of the RPD (Figure 5E).

To determine whether the reduced swimming rate of the partial RPD deletions was due to reduced number, length, or beating of cilia, we examined the morphology of cilia by immunostaining cells using polyclonal anti-tubulin antibodies. Compared with either the wild-type cells (not shown) or the cells rescued with the full-length *IFT172* (Figure 6A), cells with partially truncated *IFT172* RPD (Figure 6, B–D) contained fewer cilia and showed greater variation of cilia length within a single cell. Interestingly, the cilia density in the mutant cells was higher at the anterior part of the cells than the posterior part (Figure 6, B–D). These observations suggest that, in the cells carrying Ift172p with a partially truncated RPD, the anterograde IFT machinery required for cilia assembly is still functional, but the assembly efficiency and/or the mechanism that regulates ciliary formation or length is affected.

Ift172p with a Partial Truncation of the Repeat Domain Accumulated at the Ciliary Tip

To investigate the localization of the truncated Ift172 proteins, cells rescued with C-terminal FLAG-tagged truncated forms of *IFT172* were stained with anti-FLAG antibodies. Cells rescued with tagged or nontagged full-length constructs were not morphologically distinguishable (data not shown), indicating that the FLAG tag did not change the normal function of Ift172p.

Immunofluorescence staining revealed a striking change of the subcellular distribution of Ift172p when the RPD was partially truncated. Full-length Ift172p-FLAG localized to the cilia in a punctate manner (Figure 6A, arrow) and to the basal body. The staining could be more easily observed in the oral apparatus, which contains a high density of oral cilia (Figure 6A, Oa). The FLAG-Ift172p with a partially truncated RPD also appeared in the basal body and in the cilia, but preferentially accumulated at the distal tips of cilia (Figure 6, B–E, arrowhead). Comparing cells rescued by the constructs with different extents of truncation, we found that the preferential tip accumulation was more obvious when more of the RPD was deleted (Figure 6, B–D). This observation indicates that the C-terminal RPD plays a role in the return of Ift172p to the cell body. To further examine the distribution of truncated Ift172p during cilia biogenesis, we observed the localization of Ift172p during cilia regeneration in cells rescued with IFT172(RPDΔ3), the most truncated construct that could rescue in our study (Figure 6, F–K).

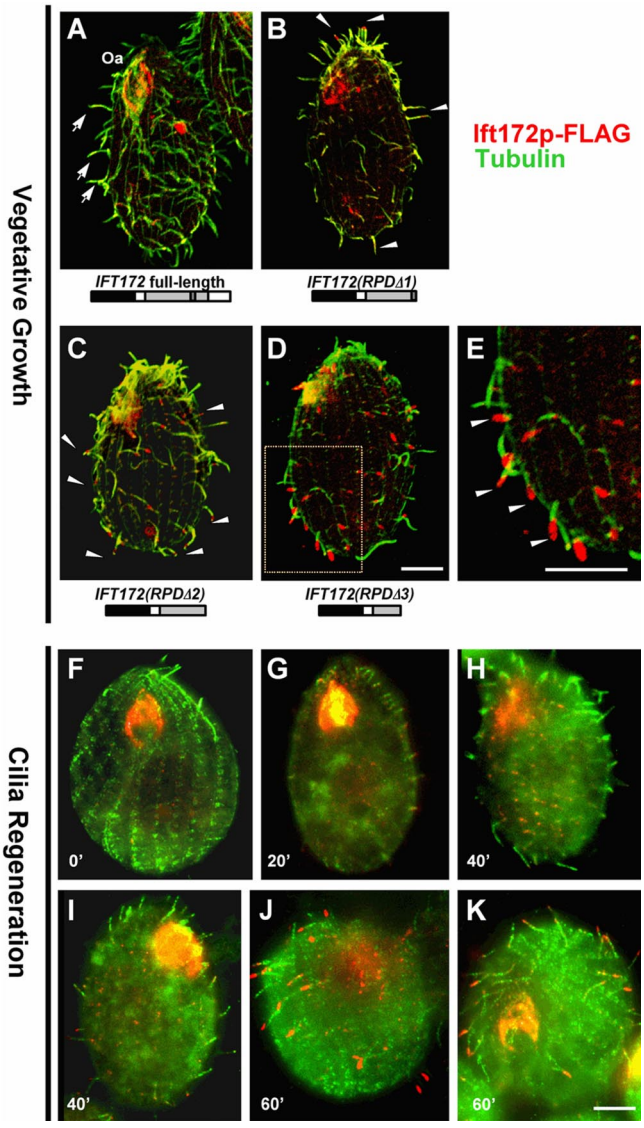

Figure 6. Morphology of the rescued cells and the localization of RPD-truncated Ift172p. (A–E) Merged confocal images of tubulin (green) and Ift172p-FLAG (red) staining on different rescued cells. The anterior end of the cell containing an oral apparatus (Oa) was positioned to the top. The diagrams below the cell images represents the truncated forms of *IFT172* used to generate the rescued knock-in cells. These FLAG-tagged truncation constructs were targeted to the *MTT1* locus. (A) Cells rescued with full-length *IFT172* showed that most of these proteins localized to the basal bodies in the cell cortex and oral apparatus, and some Ift172p-FLAG localized along the cilia (arrow). (B–E) In the cells rescued with truncated forms of *IFT172*, deletion of part of the RPD led to accumulation of the Ift172p at the distal tip of the cilia (arrowhead). (E) Higher magnification of the box region in D. Also note that cells with truncated *IFT172* assembled fewer cilia that showed increased length heterogeneity. (F–K) Fluorescent microscope images of tubulin (green) and Ift172p-FLAG (red) staining during cilia regeneration in the knocked-in cells rescued with truncated form IFT172(RPDΔ3). (F) Deciliated cell at zero time of regeneration; (G) 20 min in the recovery buffer; (H and I) 40 min in the recovery buffer; (J and K) 60 min in the recovery buffer. Bar, 100 μm.

Twenty minutes after deciliation, we observed truncated Ift172p signal in the nascent cilia (Figure 6G). RPD-truncated Ift172p continued to localize along cilia after 40 min and also

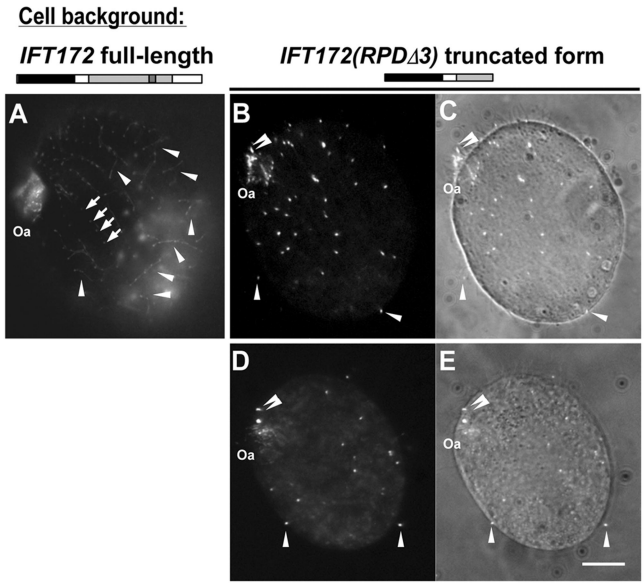

Figure 7. Localization of Ift88p-GFP in cells rescued with either full-length or RPD-truncated *IFT172*. (A) In the cells with full-length *IFT172*, Ift88p-GFP localized to oral cilia (Oa), basal body rows (arrow) and somatic cilia along the axoneme (arrowhead). (B–E) In the cells with a knocked in RPD-truncated construct IFT172(RPDΔ3), brightly fluorescent Ift88p-GFP accumulated in the cilia. The signals appeared to be enriched at the distal regions of ciliary tips, which could be observed more clearly in somatic cilia pointing out parallel to the focal plain (arrowhead) and in oral cilia (double arrowhead). (A, B, and D) Fluorescent microscope images. (C and E) Phase-contrast image merged with the fluorescent image. Bar, 10 μm.

began to show some preferential tip localization (Figure 6, H and I). After 60 min, more than half of the cells exhibited marked tip accumulation of the truncated Ift172p (Figure 6, J and K). These results show that the preferential accumulation of RPD-truncated Ift172p not only occurs in already formed cilia but also in newly assembled cilia.

Another IFT Protein Also Accumulates in the Cilia When the Ift172p Repeat Domain Was Partially Truncated

To examine whether other IFT proteins are affected by RPD-truncated Ift172p, we introduced an *IFT88* construct encoding a fused C-terminal GFP into two cell backgrounds: the *IFT172* knockout cells rescued with either the full-length *IFT172* construct or with the truncated form IFT172(RPDΔ3) (Figure 7). We then compared the localization of Ift88p-GFP in these cells. In the full-length *IFT172* rescued cells, the Ift88p-GFP mainly localized to the basal bodies (Figure 7A, arrow) and along the whole length of the cilia (Figure 7A, arrowhead). In contrast, Ift88p-GFP signals formed very bright spots in many somatic cilia of the RPD truncated cells (Figure 7, B–E). Observation of the live cells suggested that these spots tend to locate at the distal region near the ciliary tips, and this distal localization was especially obvious in oral cilia where the cilia are regularly arranged at high density (Figure 7, B–E, double arrowhead) and was more easily identified in somatic cilia pointing out at the periphery and parallel to the focal plain (Figure 7, B–E, arrowhead). This result indicates that truncation of the Ift172p RPD not only affects its own localization but also affects the spatial distribution of another IFT protein within the cell, arguing that the truncation leads to a more general defect in IFT.

DISCUSSION

Tetrahymena IFT172 knockout cells could not assemble full-length cilia, lost cell motility, and failed to complete cytokinesis. The same phenotypes were observed in *Tetrahymena IFT52* knockout cells (Brown *et al.*, 2003) and in anterograde motor kinesin-2 knockout cells (Brown *et al.*, 1999b), indicating that *IFT172*, like *IFT52*, is essential for kinesin-2–mediated anterograde transport. The involvement of *IFT172* in the assembly of functional cilia/flagella was also reported in *Chlamydomonas* (Pedersen *et al.*, 2005), *C. elegans* (Perkins *et al.*, 1986), zebrafish (Sun *et al.*, 2004), and mouse (Huangfu *et al.*, 2003). Our result and these studies show that *IFT172* is a functionally conserved gene and demonstrate the importance of IFT in cilia formation in diverse systems.

Rat SLB/IFT172 was shown to specifically repress Lhx3/4 transcriptional activity of a transfected reporter gene in cultured cells and to localize to the nucleus when cotransfected with Lhx3 (Howard and Maurer, 2000). We did not detect any *Tetrahymena* Ift172p localized in the nucleus, and a BLAST search failed to identify Lhx3 orthologues in the *Tetrahymena* macronuclear genome. Thus, although we cannot exclude the possibility that an undetectable level of nuclear Ift172p modulates unidentified transcriptional factors, it remains possible that *Tetrahymena* Ift172p sequesters transcriptional factors in the cytoplasm, within, or at the base of the cilia to regulate gene expression without entering the nucleus. However, because deletion of the *Tetrahymena* Ift172p repeat unit corresponding to the LIM-ID on rat SLB did not cause discernable defects in cell growth or ciliary function, a more likely alternative explanation of the discrepancy is that the regulatory activities of rat SLB are more recently derived functions that evolved in addition to its conserved role in IFT. If so, however, the reason the repeat homologous to the LIM-ID is conserved in *Tetrahymena* remains unknown.

In addition to the essential anterograde transport function shared with other complex B proteins (Scholey, 2003), our studies indicate that *IFT172* is also involved in other steps of IFT. Ift172p with a partially truncated RPD preferentially accumulated at the ciliary tip and caused at least one other IFT protein to do likewise. Because distal tip accumulation of ciliary proteins is a phenotype characteristic of defective retrograde IFT (Pazour *et al.*, 1998, 1999), our observations argue that *IFT172* is either involved in the retrograde process or is required immediately upstream of retrograde IFT for the anterograde/retrograde turnaround at the ciliary tips (Pedersen *et al.*, 2005, 2006). A microscopic analysis of the movement of GFP-tagged Ift172p within the cilia of living cells would differentiate the two steps, but lack of a *Tetrahymena* mutant bearing completely nonmotile cilia precludes us from observing the intraciliary motility to address this issue directly.

Recent biochemical studies on *Chlamydomonas* IFT proteins imply that *IFT172* may play a role in the IFT remodeling at the tip. During in vitro extraction of the *Chlamydomonas* IFT complex, IFT172 dissociated from other Complex B proteins at relatively mild ionic strength, suggesting that IFT172 might dissociate from the rest of the complex more easily in vivo and change the configuration of the complex (Cole *et al.*, 1998; Lucker *et al.*, 2005). Importantly, Pedersen *et al.* (2005) showed that *Chlamydomonas* EB1, a MT plus-end binding protein that localizes at the flagella tip, physically interacts with a fraction of IFT172 proteins that are not associated with other IFT components. Our observations and these results collectively argue that, in addition to its essential role in the anterograde transport, *IFT172* is also

most likely involved in the anterograde/retrograde transition mediated by ciliary tip proteins.

Tetrahymena IFT172 and its orthologues share a similar domain organization, which contains a beta strand–rich WDD at the N-terminus and an alpha helix–rich RPD at the C-terminus. The WDD contains WD40 motifs known for protein–protein interaction (Smith *et al.,* 1999). The RPD is mainly composed of degenerate repeats. Although the exact function of the RPD is not clear, each repeat unit could be superimposed to three or four alpha helices, indicating that it could form a regular structural module and possibly serves as a scaffold to interact with other IFT proteins, cargo, or regulatory factors.

Putative protein–protein interaction motifs are predicted from the sequences in almost every IFT protein (Cole, 2003), but the physiological roles of these motifs and their interactions during the IFT processes remain unclear. Recent studies have begun to identify interacting partners among the IFT proteins and map the regions required for binding. Mammalian IFT20 interacts with IFT57 in the yeast two-hybrid assay through the coiled-coil domains on both proteins (Baker *et al.,* 2003). Two-hybrid and chemical cross-linking assays showed that the coiled-coil regions of *Chlamydomonas* IFT81 and IFT74/72 were required to form the core of IFT complex B (Lucker *et al.,* 2005). Taking advantages of the facile gene targeting in *Tetrahymena,* we used an alternative approach to generate "knock-in" cells with various deletion forms of *IFT172* and examined the phenotype of these mutant cells, so that the in vivo function of the protein–protein interaction domains could be inferred (see Figure 8).

The constructs containing either the WDD or the RPD alone failed to rescue the *IFT172* knockout cells and could not target to the cilia or to basal bodies, the proposed docking and assembly site of the IFT complex (Deane *et al.,* 2001), indicating that both domains are required for the localization and function of Ift172p. At the base of the cilia, a selectively gated entry of the proteins from the cell body into the ciliary compartment has been proposed (Rosenbaum and Witman, 2002). Because both the WDD and RPD are required for Ift172p to localize to cilia, we postulate that both domains are utilized cooperatively to interact with protein factors at the basal body and/or to assemble Ift172p into a functional complex that is required for entry into cilia (Figure 8, Step 1). An evolutionary analysis of IFT proteins proposed a common origin of IFT and the coated-vesicle–mediated transport system (Jekely and Arendt, 2006). Vesicle coat components, such as COPI and clathrin, and some IFT proteins, including *IFT172,* share a two-domain structural feature that was hypothesized to mediate a sorting mechanism. Proteomic analyses of the proteins that coimmunoprecipitate with the two individual Ift172p domains expressed in vivo could help to reveal details of these interactions.

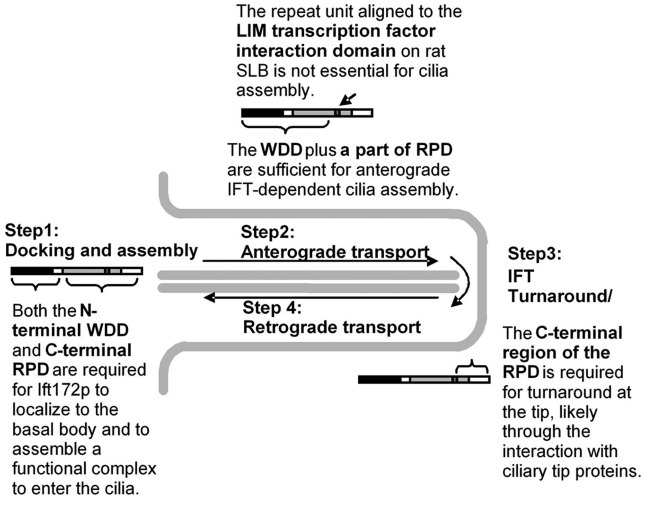

Figure 8. Summary of Ift172p functional domains involved in the IFT process.

Tetrahymena with a partial deletion of the Ift172p RPD could grow cilia, indicating that a complete RPD is not essential, whereas the WDD plus a minimal region of RPD is sufficient for anterograde IFT (Figure 8, Step 2). However, partial truncations of the RPD caused aberrant accumulations of truncated Ift172p itself and of Ift88p at the ciliary tip. These observations argue that the turnaround at the tip (Figure 8, Step 3) and/or the retrograde transport of IFT proteins (Figure 8, Step 4) requires the presence of multiple repeats in the RPD of Ift172p to function efficiently.

The *IFT172* RPD may affect the return of the IFT proteins from the ciliary tip by several possible means. One is that the RPD contains the sites that attach Ift172p to the retrograde motors and associated IFT-B proteins. In this scenario, truncation does not necessarily affect the remodeling/retrograde machinery per se but abolishes the loading of IFT-B proteins to the cytoplasmic dynein and hence interferes the return of IFT proteins indirectly. Alternatively, Ift172p may interact with other factors or ciliary tip proteins through the RPD during IFT remodeling/turnaround. At the very end of the *Tetrahymena* ciliary tip, the extension of the outer doublet axonemal MTs become singlets (Dentler, 1984). In *C. elegans*, the more prominent distal segments of sensory cilia also contain singlet MTs, and their assembly requires a homodimeric kinesin-2, Osm-3 (Snow *et al.,* 2004). A mitogen-activated protein (MAP) kinase, Dyf-5, is responsible for restricting the heterotrimeric kinesin-II from entering into the distal segment (Burghoorn *et al.,* 2007). Loss-of-function of Dyf-5 causes long cilia and accumulation of IFT proteins within the cilia (Burghoorn *et al.,* 2007). The *Tetrahymena OSM-3* homolog has been cloned (Awan *et al.,* 2004) and a putative Dyf-5 ortholog is present in the macronuclear genome, but their physiological roles are not known. It would be interesting to check if any interaction exists between Ift172p RPD and these proteins at the distal ciliary tip.

Protein accumulation at the flagellar tip was observed in the *Chlamydomonas* IFT172 mutant *fla11*, in which a single residue substitution occurred in the repeat nearest to the C-terminus (Pedersen *et al.,* 2005). *Chlamydomonas* wild-type IFT172 and EB1 proteins could interact with each other and the ultrastructure at the flagellar tip is altered in *fla11* cells, suggesting the interaction between IFT and the ciliary tip complex proteins is direct and functionally important (Pedersen *et al.,* 2005). Unlike *Chlamydomonas* that possesses only one EB1 gene (Pedersen *et al.,* 2003), seven likely EB1 orthologues were identified in the *Tetrahymena* macronuclear genome (Eisen *et al.,* 2006), and it will be difficult to determine whether one or all of these interact with Ift172p. Given that the phenotype observed in our *IFT172* RPD-truncated mutant is similar to *fla11*, we speculate that the interaction between Ift172p and EB1 is mediated through the C-terminal RPD of Ift172p (Figure 8, Step 3) in a manner that depends on the number of repeats.

ACKNOWLEDGMENTS

We thank Josephine Bowen for technical assistance. This work was supported by National Institutes of Health Grant GM-26973.

REFERENCES

Andrade, M. A., Ponting, C. P., Gibson, T. J., and Bork, P. (2000). Homology-based method for identification of protein repeats using statistical significance estimates. J. Mol. Biol. *298*, 521–537.

Awan, A., Bernstein, M., Hamasaki, T., and Satir, P. (2004). Cloning and characterization of Kin5, a novel *Tetrahymena* ciliary kinesin II. Cell Motil. Cytoskelet. *58*, 1–9.

Baker, S. A., Freeman, K., Luby-Phelps, K., Pazour, G. J., and Besharse, J. C. (2003). IFT20 links kinesin II with a mammalian intraflagellar transport complex that is conserved in motile flagella and sensory cilia. J. Biol. Chem. *278*, 34211–34218.

Bell, L. R., Stone, S., Yochem, J., Shaw, J. E., and Herman, R. K. (2006). The molecular identities of the *Caenorhabditis elegans* intraflagellar transport genes dyf-6, daf-10 and osm-1. Genetics *173*, 1275–1286.

Brazelton, W. J., Amundsen, C. D., Silflow, C. D., and Lefebvre, P. A. (2001). The bld1 mutation identifies the *Chlamydomonas* osm-6 homolog as a gene required for flagellar assembly. Curr. Biol. *11*, 1591–1594.

Brown, J. M., Fine, N. A., Pandiyan, G., Thazhath, R., and Gaertig, J. (2003). Hypoxia regulates assembly of cilia in suppressors of *Tetrahymena* lacking an intraflagellar transport subunit gene. Mol. Biol. Cell *14*, 3192–3207.

Brown, J. M., Hardin, C., and Gaertig, J. (1999a). Rotokinesis, a novel phenomenon of cell locomotion-assisted cytokinesis in the ciliate *Tetrahymena thermophila.* Cell Biol. Int. *23*, 841–848.

Brown, J. M., Marsala, C., Kosoy, R., and Gaertig, J. (1999b). Kinesin-II is preferentially targeted to assembling cilia and is required for ciliogenesis and normal cytokinesis in *Tetrahymena.* Mol. Biol. Cell *10*, 3081–3096.

Burghoorn, J., Dekkers, M. P., Rademakers, S., de Jong, T., Willemsen, R., and Jansen, G. (2007). Mutation of the MAP kinase DYF-5 affects docking and undocking of kinesin-2 motors and reduces their speed in the cilia of *Caenorhabditis elegans.* Proc. Natl. Acad. Sci. USA *104*, 7157–7162.

Calzone, F. J., and Gorovsky, M. A. (1982). Cilia regeneration in *Tetrahymena.* A simple reproducible method for producing large numbers of regenerating cells. Exp. Cell Res. *140*, 471–476.

Cassidy-Hanley, D., Bowen, J., Lee, J. H., Cole, E., VerPlank, L. A., Gaertig, J., Gorovsky, M. A., and Bruns, P. J. (1997). Germline and somatic transformation of mating *Tetrahymena thermophila* by particle bombardment. Genetics *146*, 135–147.

Cole, D. G. (2003). The intraflagellar transport machinery of *Chlamydomonas reinhardtii.* Traffic *4*, 435–442.

Cole, D. G., Chinn, S. W., Wedaman, K. P., Hall, K., Vuong, T., and Scholey, J. M. (1993). Novel heterotrimeric kinesin-related protein purified from sea urchin eggs. Nature *366*, 268–270.

Cole, D. G., Diener, D. R., Himelblau, A. L., Beech, P. L., Fuster, J. C., and Rosenbaum, J. L. (1998). *Chlamydomonas* kinesin-II-dependent intraflagellar transport (IFT): IFT particles contain proteins required for ciliary assembly in *Caenorhabditis elegans* sensory neurons. J. Cell Biol. *141*, 993–1008.

Deane, J. A., Cole, D. G., Seeley, E. S., Diener, D. R., and Rosenbaum, J. L. (2001). Localization of intraflagellar transport protein IFT52 identifies basal body transitional fibers as the docking site for IFT particles. Curr. Biol. *11*, 1586–1590.

Dentler, W. L. (1984). Attachment of the cap to the central microtubules of *Tetrahymena* cilia. J. Cell Sci. *66*, 167–173.

Dou, Y., Song, X., Liu, Y., and Gorovsky, M. A. (2005). The H1 phosphorylation state regulates expression of CDC2 and other genes in response to starvation in *Tetrahymena thermophila.* Mol. Cell. Biol. *25*, 3914–3922.

Eisen, J. A. *et al.* (2006). Macronuclear genome sequence of the ciliate *Tetrahymena thermophila*, a model eukaryote. PLoS Biol. *4*, e286.

Frankel, J. (2000). Cell biology of *Tetrahymena thermophila.* Methods Cell Biol. *62*, 27–125.

Gaertig, J. (2000). Molecular mechanisms of microtubular organelle assembly in *Tetrahymena.* J. Eukaryot. Microbiol. *47*, 185–190.

Gaertig, J., Gu, L., Hai, B., and Gorovsky, M. A. (1994). High frequency vector-mediated transformation and gene replacement in *Tetrahymena.* Nucleic Acids Res. *22*, 5391–5398.

Gorovsky, M. A., Yao, M. C., Keevert, J. B., and Pleger, G. L. (1975). Isolation of micro- and macronuclei of *Tetrahymena pyriformis.* Methods Cell Biol. *9*, 311–327.

Gurskaya, N. G., Diatchenko, L., Chenchik, A., Siebert, P. D., Khaspekov, G. L., Lukyanov, K. A., Vagner, L. L., Ermolaeva, O. D., Lukyanov, S. A., and Sverdlov, E. D. (1996). Equalizing cDNA subtraction based on selective suppression of polymerase chain reaction: cloning of Jurkat cell transcripts induced by phytohemaglutinin and phorbol 12-myristate 13-acetate. Anal. Biochem. *240*, 90–97.

Guttman, S. D., and Gorovsky, M. A. (1979). Cilia regeneration in starved tetrahymena: an inducible system for studying gene expression and organelle biogenesis. Cell *17*, 307–317.

Hai, B., Gaertig, J., and Gorovsky, M. A. (2000). Knockout heterokaryons enable facile mutagenic analysis of essential genes in *Tetrahymena.* Methods Cell Biol. *62*, 513–531.

Hai, B., and Gorovsky, M. A. (1997). Germ-line knockout heterokaryons of an essential alpha-tubulin gene enable high-frequency gene replacement and a test of gene transfer from somatic to germ-line nuclei in *Tetrahymena thermophila.* Proc. Natl. Acad. Sci. USA *94*, 1310–1315.

Haycraft, C. J., Banizs, B., Aydin-Son, Y., Zhang, Q., Michaud, E. J., and Yoder, B. K. (2005). Gli2 and gli3 localize to cilia and require the intraflagellar transport protein polaris for processing and function. PLoS Genet. *1*, e53.

Haycraft, C. J., Schafer, J. C., Zhang, Q., Taulman, P. D., and Yoder, B. K. (2003). Identification of CHE-13, a novel intraflagellar transport protein required for cilia formation. Exp. Cell Res. *284*, 251–263.

Haycraft, C. J., Swoboda, P., Taulman, P. D., Thomas, J. H., and Yoder, B. K. (2001). The *C. elegans* homolog of the murine cystic kidney disease gene Tg737 functions in a ciliogenic pathway and is disrupted in osm-5 mutant worms. Development *128*, 1493–1505.

Hou, Y., Qin, H., Follit, J. A., Pazour, G. J., Rosenbaum, J. L., and Witman, G. B. (2007). Functional analysis of an individual IFT protein: IFT46 is required for transport of outer dynein arms into flagella. J. Cell Biol. *176*, 653–665.

Howard, P. W., and Maurer, R. A. (2000). Identification of a conserved protein that interacts with specific LIM homeodomain transcription factors. J. Biol. Chem. *275*, 13336–13342.

Huangfu, D., and Anderson, K. V. (2005). Cilia and Hedgehog responsiveness in the mouse. Proc. Natl. Acad. Sci. USA *102*, 11325–11330.

Huangfu, D., Liu, A., Rakeman, A. S., Murcia, N. S., Niswander, L., and Anderson, K. V. (2003). Hedgehog signalling in the mouse requires intraflagellar transport proteins. Nature *426*, 83–87.

Iomini, C., Babaev-Khaimov, V., Sassaroli, M., and Piperno, G. (2001). Protein particles in *Chlamydomonas* flagella undergo a transport cycle consisting of four phases. J. Cell Biol. *153*, 13–24.

Jekely, G., and Arendt, D. (2006). Evolution of intraflagellar transport from coated vesicles and autogenous origin of the eukaryotic cilium. Bioessays *28*, 191–198.

Johnson, K. A., and Rosenbaum, J. L. (1992). Polarity of flagellar assembly in *Chlamydomonas.* J. Cell Biol. *119*, 1605–1611.

Kozminski, K. G., Beech, P. L., and Rosenbaum, J. L. (1995). The *Chlamydomonas* kinesin-like protein FLA10 is involved in motility associated with the flagellar membrane. J. Cell Biol. *131*, 1517–1527.

Kozminski, K. G., Johnson, K. A., Forscher, P., and Rosenbaum, J. L. (1993). A motility in the eukaryotic flagellum unrelated to flagellar beating. Proc. Natl. Acad. Sci. USA *90*, 5519–5523.

Lawrence, C. J. *et al.* (2004). A standardized kinesin nomenclature. J. Cell Biol. *167*, 19–22.

Liao, J., Chan, C. H., and Gong, Z. (1997). An alternative linker-mediated polymerase chain reaction method using a dideoxynucleotide to reduce amplification background. Anal. Biochem. *253*, 137–139.

Liu, Y., Mochizuki, K., and Gorovsky, M. A. (2004). Histone H3 lysine 9 methylation is required for DNA elimination in developing macronuclei in *Tetrahymena.* Proc. Natl. Acad. Sci. USA *101*, 1679–1684.

Lucker, B. F., Behal, R. H., Qin, H., Siron, L. C., Taggart, W. D., Rosenbaum, J. L., and Cole, D. G. (2005). Characterization of the intraflagellar transport complex B core: direct interaction of the IFT81 and IFT74/72 subunits. J. Biol. Chem. *280*, 27688–27696.

Marshall, W. F., Qin, H., Rodrigo Brenni, M., and Rosenbaum, J. L. (2005). Flagellar length control system: testing a simple model based on intraflagellar transport and turnover. Mol. Biol. Cell *16*, 270–278.

Marshall, W. F., and Rosenbaum, J. L. (2001). Intraflagellar transport balances continuous turnover of outer doublet microtubules: implications for flagellar length control. J. Cell Biol. *155*, 405–414.

May, S. R., Ashique, A. M., Karlen, M., Wang, B., Shen, Y., Zarbalis, K., Reiter, J., Ericson, J., and Peterson, A. S. (2005). Loss of the retrograde motor for IFT disrupts localization of Smo to cilia and prevents the expression of both activator and repressor functions of Gli. Dev. Biol. *287*, 378–389.

Orias, E., and Rasmussen, L. (1976). Dual capacity for nutrient uptake in *Tetrahymena*. IV. Growth without food vacuoles and its implications. Exp. Cell Res. *102*, 127–137.

Pan, X., Ou, G., Civelekoglu-Scholey, G., Blacque, O. E., Endres, N. F., Tao, L., Mogilner, A., Leroux, M. R., Vale, R. D., and Scholey, J. M. (2006). Mechanism of transport of IFT particles in *C. elegans* cilia by the concerted action of kinesin-II and OSM-3 motors. J. Cell Biol. *174*, 1035–1045.

Pazour, G. J., Baker, S. A., Deane, J. A., Cole, D. G., Dickert, B. L., Rosenbaum, J. L., Witman, G. B., and Besharse, J. C. (2002). The intraflagellar transport protein, IFT88, is essential for vertebrate photoreceptor assembly and maintenance. J. Cell Biol. *157*, 103–113.

Pazour, G. J., Dickert, B. L., Vucica, Y., Seeley, E. S., Rosenbaum, J. L., Witman, G. B., and Cole, D. G. (2000). *Chlamydomonas* IFT88 and its mouse homologue, polycystic kidney disease gene tg737, are required for assembly of cilia and flagella. J. Cell Biol. *151*, 709–718.

Pazour, G. J., Dickert, B. L., and Witman, G. B. (1999). The DHC1b (DHC2) isoform of cytoplasmic dynein is required for flagellar assembly. J. Cell Biol. *144*, 473–481.

Pazour, G. J., Wilkerson, C. G., and Witman, G. B. (1998). A dynein light chain is essential for the retrograde particle movement of intraflagellar transport (IFT). J. Cell Biol. *141*, 979–992.

Pedersen, L. B., Geimer, S., and Rosenbaum, J. L. (2006). Dissecting the molecular mechanisms of intraflagellar transport in *Chlamydomonas*. Curr. Biol. *16*, 450–459.

Pedersen, L. B., Geimer, S., Sloboda, R. D., and Rosenbaum, J. L. (2003). The Microtubule plus end-tracking protein EB1 is localized to the flagellar tip and basal bodies in *Chlamydomonas reinhardtii*. Curr. Biol. *13*, 1969–1974.

Pedersen, L. B., Miller, M. S., Geimer, S., Leitch, J. M., Rosenbaum, J. L., and Cole, D. G. (2005). *Chlamydomonas* IFT172 is encoded by FLA11, interacts with CrEB1, and regulates IFT at the flagellar tip. Curr. Biol. *15*, 262–266.

Perkins, L. A., Hedgecock, E. M., Thomson, J. N., and Culotti, J. G. (1986). Mutant sensory cilia in the nematode *Caenorhabditis elegans*. Dev. Biol. *117*, 456–487.

Qin, H., Diener, D. R., Geimer, S., Cole, D. G., and Rosenbaum, J. L. (2004). Intraflagellar transport (IFT) cargo: IFT transports flagellar precursors to the tip and turnover products to the cell body. J. Cell Biol. *164*, 255–266.

Qin, H., Wang, Z., Diener, D., and Rosenbaum, J. (2007). Intraflagellar transport protein 27 is a small G protein involved in cell-cycle control. Curr. Biol. *17*, 193–202.

Robert, A., Margall-Ducos, G., Guidotti, J. E., Bregerie, O., Celati, C., Brechot, C., and Desdouets, C. (2007). The intraflagellar transport component IFT88/polaris is a centrosomal protein regulating G1-S transition in non-ciliated cells. J. Cell Sci. *120*, 628–637.

Rosenbaum, J. L., and Carlson, K. (1969). Cilia regeneration in *Tetrahymena* and its inhibition by colchicine. J. Cell Biol. *40*, 415–425.

Rosenbaum, J. L., and Witman, G. B. (2002). Intraflagellar transport. Nat. Rev. Mol. Cell Biol. *3*, 813–825.

Sarpal, R., Todi, S. V., Sivan-Loukianova, E., Shirolikar, S., Subramanian, N., Raff, E. C., Erickson, J. W., Ray, K., and Eberl, D. F. (2003). *Drosophila* KAP interacts with the kinesin II motor subunit KLP64D to assemble chordotonal sensory cilia, but not sperm tails. Curr. Biol. *13*, 1687–1696.

Scholey, J. M. (2003). Intraflagellar transport. Annu. Rev. Cell Dev. Biol. *19*, 423–443.

Schultz, J., Milpetz, F., Bork, P., and Ponting, C. P. (1998). SMART, a simple modular architecture research tool: identification of signaling domains. Proc. Natl. Acad. Sci. USA *95*, 5857–5864.

Shang, Y., Li, B., and Gorovsky, M.A. (2002a). Tetrahymena thermophila contains a conventional gamma-tubulin that is differentially required for the maintenance of different microtubule-organizing centers. J. Cell Biol. *158*, 1195–1206.

Shang, Y., Song, X., Bowen, J., Corstanje, R., Gao, Y., Gaertig, J., and Gorovsky, M. A. (2002b). A robust inducible-repressible promoter greatly facilitates gene knockouts, conditional expression, and overexpression of homologous and heterologous genes in *Tetrahymena thermophila*. Proc. Natl. Acad. Sci. USA *99*, 3734–3739.

Signor, D., Wedaman, K. P., Orozco, J. T., Dwyer, N. D., Bargmann, C. I., Rose, L. S., and Scholey, J. M. (1999). Role of a class DHC1b dynein in retrograde transport of IFT motors and IFT raft particles along cilia, but not dendrites, in chemosensory neurons of living *Caenorhabditis elegans*. J. Cell Biol. *147*, 519–530.

Sleigh, M. A. (1974). Cilia and Flagella, New York: Academic Press.

Smith, T. F., Gaitatzes, C., Saxena, K., and Neer, E. J. (1999). The WD repeat: a common architecture for diverse functions. Trends Biochem. Sci. *24*, 181–185.

Snow, J. J., Ou, G., Gunnarson, A. L., Walker, M. R., Zhou, H. M., Brust-Mascher, I., and Scholey, J. M. (2004). Two anterograde intraflagellar transport motors cooperate to build sensory cilia on *C. elegans* neurons. Nat. Cell Biol. *6*, 1109–1113.

Stuart, K. R., and Cole, E. S. (2000). Nuclear and cytoskeletal fluorescence microscopy techniques. Methods Cell Biol. *62*, 291–311.

Sun, Z., Amsterdam, A., Pazour, G. J., Cole, D. G., Miller, M. S., and Hopkins, N. (2004). A genetic screen in zebrafish identifies cilia genes as a principal cause of cystic kidney. Development *131*, 4085–4093.

Thompson, J. D., Gibson, T. J., Plewniak, F., Jeanmougin, F., and Higgins, D. G. (1997). The CLUSTALX windows interface: flexible strategies for multiple sequence alignment aided by quality analysis tools. Nucleic Acids Res. *25*, 4876–4882.

Van De Water, L., 3rd, Guttman, S. D., Gorovsky, M. A., and Olmsted, J. B. (1982). Production of antisera and radioimmunoassays for tubulin. Methods Cell Biol. *24*, 79–96.

Wang, Q., Pan, J., and Snell, W. J. (2006). Intraflagellar transport particles participate directly in cilium-generated signaling in *Chlamydomonas*. Cell *125*, 549–562.

Wicks, S. R., de Vries, C. J., van Luenen, H. G., and Plasterk, R. H. (2000). CHE-3, a cytosolic dynein heavy chain, is required for sensory cilia structure and function in *Caenorhabditis elegans*. Dev. Biol. *221*, 295–307.

Xie, R., Clark, K. M., and Gorovsky, M. A. (2007). Endoplasmic reticulum retention signal-dependent glycylation of the hsp70/grp170-related Pgp1p in *Tetrahymena*. Eukaryot. Cell *6*, 388–397.

Yao, M. C., and Yao, C. H. (1991). Transformation of *Tetrahymena* to cycloheximide resistance with a ribosomal protein gene through sequence replacement. Proc. Natl. Acad. Sci. USA *88*, 9493–9497.